Article:

Qiu, S, Yang, H, Zhang, S et al. (10 more authors) (2023) Carbon storage in an arable soil combining field measurements, aggregate turnover modeling and climate scenarios. Catena, 220 (Part A). 106708. p. 106708. ISSN 0341-8162

https://doi.org/10.1016/j.catena.2022.106708

Carbon storage in an arable soil combining field measurements, aggregate turnover modeling and climate scenarios

Shaojun Qiu[a], Huiyi Yang[b], Shuiqing Zhang[c], Shaomin Huang[c], Shicheng Zhao[a], Xingpeng Xu[a], Ping He[a,*], Wei Zhou[a], Ying Zhao[d,*], Na Yan[e], Nikolaos Nikolaidis[f], Peter Christie[a], Steven A Banwart[e]

[a]Key Laboratory of Plant Nutrition and Fertilizers, Ministry of Agriculture; Institute of Agricultural Resources and Regional Planning, Chinese Academy of Agricultural Sciences, Beijing 100081, China

[b]Natural Resources Institute, University of Greenwich, Central Avenue, Chatham Maritime ME4 4TB, Kent, UK

[c]Institute of Plant Nutrition and Environmental Resources, Henan Academy of Agricultural Sciences, Zhengzhou 450002, China

[d]College of Resources and Environmental Engineering, Ludong University, Yantai 264025, China

[e]Global Food and Environment Institute and School of Earth and Environment, University of Leeds, Leeds LS2 9JT, United Kingdom

[f]School of Environmental Engineering, Technical University of Crete, Crete 73100, Greece

[*] Corresponding author: P. He or Y. Zhao. E-mail: heping02@caas.cn or yzhaosoils@gmail.com, Tel: +86-10-82105638; Fax: +86-10-82106206.

Abstract

Quantifying soil structural dynamics and aggregate turnover is important in understanding soil organic carbon (SOC) stocks, particularly over decadal and larger time scales. Until now it has remained unclear clear how soil aggregate size and its associated carbon respond to both long-term soil fertility and climate change. Here, we explore changes in soil structure and aggregate organic C (OC) stocks under different fertilization practices by combining field chronosequence SOC measurements with dynamic and process modeling in a long-term wheat-maize field experiment on the North China Plain. The fertilization practices comprise no fertilization (CK), chemical fertilization (NPK), and combined manure and NPK treatments (MNPK). The experimental measurements included the mass of OC stocks in different soil aggregate size classes. We used this information to calibrate parameters of the Carbon, Aggregation, and Structure Turnover (CAST) model and to predict future changes in aggregate structure and the resulting OC stocks using the RCP2.6 scenarios that were defined by the outputs of five future climate models from IPCC projection. With trends towards a wetter climate and increasing soil moisture under the RCP2.6 scenarios for the region, soil OC stocks will increase in all three treatments, with the strongest increase under MNPK due to exogenous C inputs. The CAST model output further suggests that changes in microaggregate (250-53 μm) OC stocks in the NPK and MNPK treatments accounted for 78.6% and 75.3% of the calculated change in total SOC stocks between the early and late 21st century. In conclusion, our combined data and modeling approach describes changes in soil aggregate C, identifies the primary soil aggregate size class of microaggregates involved in C sequestration in an agricultural soil, and predicts the role of Fluvaquent soils on the North China Plain as a future C sink.

Keywords: Organic C stocks; fertilizer practices; model simulation; RCP2.6 scenarios; soil aggregates

1. Introduction

The potential for soil organic carbon (SOC) accumulation to slow down or reverse climate warming has become a topic of considerable interest (Carvalhais et al., 2014; Baveye et al., 2018; Poulton et al., 2018). Physical protection of soil aggregates is critical for SOC storage (Six and Paustian, 2014) and mineral protected C is essential for long-term SOC turnover. The C stocks within soil aggregates in agricultural soils are influenced by management practices such as tillage and application of chemical fertilizers or exogenous C. However, our understanding and prediction of soil C kinetics remain limited, especially the response of different soil aggregate C fractions under different fertilization practices to climate change.

Organic manure or chemical fertilizer applications are important fertilization practices. Organic manures and fertilizers can also provide additional soil C inputs. Chemical fertilizers can increase SOC by increasing net plant productivity or plant residues or by suppressing the biological activity of the soil decomposer microbial community (Treseder, 2008; Brown et al., 2014; Averill and Waring, 2018) or can decrease SOC by increasing SOC mineralization (Russel et al., 2009). These processes occur over different time-scales and may not persist beyond episodic or seasonal effects, making long-term SOC predictions difficult. The SOC reservoir is often split into distinct pools defined by sources and decomposition pathways that exhibit characteristic residence times to facilitate the interpretation of results from field studies. Current mathematical models of SOC decomposition usually characterize these different pools using factors that impact decomposition rates, with labile SOC pools playing a key role in short-term C cycling and recalcitrant pools determining the magnitude of long-term C stocks (Zhou et al., 2018). However, new insights into the factors that define SOC pools and decomposition pathways and rates are leading to new conceptual models of SOC dynamics that consider more strongly the role of soil aggregates and of fungal and bacterial biomass in storing and processing SOC (Banwart et al., 2019).

Aggregates are the structural units in soils that largely control SOC dynamics (Six and Paustian, 2014). Correspondingly, C storage in different aggregate size classes reflects the physical, chemical, and biochemical mechanisms that protect SOC (Six et al., 2002b; Six and Paustian, 2014). The accumulation or loss of SOC is determined by macroaggregate turnover, i.e., the relative persistence of aggregates as they form and disintegrate, microaggregate formation, C stabilization within microaggregates, and their incorporation into macroaggregates (Six et al, 2000a; Gulde et al., 2008). Particulate organic matter (POM) can act as a nucleus for aggregate formation (Gulde et al., 2008) by selecting for active microbial decomposer communities that support biofilm development and potentially help bind textural units to the POM (Banwart et al., 2019). The exogenous C derived from the application of crop residues or organic manures in agricultural soils provides a binding agent for aggregate formation with possible consequences for long-term C storage (Bronick and Lal, 2005). However, the frequent removal of aboveground biomass and soil disturbance through tillage cause temporal variability in soil C dynamics, making it difficult to do long-term evaluations based on field experiments alone. Mathematical models of soil C dynamics have therefore become indispensable in evaluating and predicting changes in soil OC stocks in agricultural soils (Coleman and Jenkinson, 1999; Keating et al., 2003; Malamoud et al., 2009).

Stamati et al. (2013) recently developed a coupled C, aggregation and structure turnover (CAST) model which integrates a conceptual model of aggregate formation (Gulde et al., 2008) and its formulation as a mathematical model for soil structure dynamics (Struc-C model) (Malamoud et al., 2009) with a model of SOC turnover and plant litter inputs developed from the Rothamsted long-term field experiments (RothC model) (Coleman and Jenkinson, 1999). The CAST model considers the C contents within macroaggregate, microaggregate, and silt-clay unit size aggregates as contributions to the total SOC pool (Stamati et al. 2013; Apostolakis et al., 2017; Li et al., 2017) and simulates the formation and disintegration rate of each aggregate size class in response to C inputs and feedbacks on SOC dynamics in non-waterlogged surface soils. The CAST model can also be used to explore the C dynamics of different aggregate size classes in soils and to predict the scale and rate of response of soil structure and aggregate C dynamics to management practices and climate change.

Fluvaquent soils are the dominant soil type on the North China Plain. The region is the second largest alluvial plain in the country, formed mainly by sedimentary deposits of the lower basin of the Yellow River flowing through the central plain to the Bohai Sea on the east coast, and is bounded on the west, east and north by low mountain ranges. Mechanized, largely intensive, agriculture is the dominant land use outside of urban centers. This region is a strategic national agricultural resource contributing > 30% of national grain production to food security, over half the wheat and one-third of the total Chinese maize production (Han et al., 2018). Fluvaquent soils on the North China Plain account for 53% of the total Chinese area of Fluvaquent soils and have low SOC contents that have increased noticeably since the 1980s as a result of intensive agronomic management practices (Huang and Sun, 2006; Han et al., 2018). Several studies on Fluvaquent soils have found that OC stocks in soil aggregate size classes can be increased by applications of manures and chemical fertilizers (Yan et al., 2012; He et al., 2015). However, the mechanisms underlying C stabilization in the various aggregate size classes and the potential for long-term C sequestration in response to climate change in these soils remain unclear.

It is anticipated that changes in temperature and precipitation throughout the 21st century (IPCC, 2014) will add further uncertainty to long-term estimates of soil C storage. So far, manipulative warming studies do not point to a clear pattern in soil C responses (van Gestel et al., 2018). It is promising that integrating data with process-based models might increase our understanding of soil C dynamics in a changing climate (van Gestel et al., 2018; Valkama et al., 2020). Some studies report that the predicted SOC sequestration of Fluvaquent soils to the late 21st century will increase in most future climate scenarios (Jiang et al., 2014; Zhang et al., 2016) but it remains unclear how SOC and soil structure dynamics may interact to influence both C accumulation and changes in soil structure and thus fertility, and how to increase these through intervention with favorable agronomic practices in the long term.

To address these questions we hypothesize that (1) the increases in SOC and soil aggregate C contents under combined manure and chemical fertilizer applications can effectively contribute to the persistent sequestration of C in agricultural soils and thus help to mitigate global warming, (2) microaggregates within macroaggregates are the major soil fractions involved in C accumulation or loss under climate warming. The aims of the present study were therefore to (1) quantify the dynamics of different soil aggregate size classes and their associated OC stocks and (2) make century-scale projections of SOC change in the different aggregate size classes in response to climate warming and fertilizer treatments. We illustrate our study by combining results from a 24-year-old long-term fertilization experiment with a wheat-maize rotation on a Fluvaquent soil, future climate scenarios, and CAST soil modeling to provide new insights into the role of soil aggregates in determining long-term changes in soil C and structure dynamics.

2. Materials and methods

2.1. Soil and site description

Fluvaquent soils on the North China Plain (32 - 40°N, 114 - 121°E) experience warm temperate continental monsoon conditions and the soil type is Calcaric Cambisol (FAO classification). The study site is located on the southern part of the North China Plain in Zhengzhou, Henan province (34°47'N, 113°40'E). The mean annual temperature is 15 °C and the annual frost-free period is 175 to 220 days. Annual precipitation is 500-900 mm with 50-75% of the rainfall occurring during summer (July-September). The field experiment started in October 1990 with the prevalent local intensive double season cropping per year with an annual rotation of winter wheat and summer maize. Winter wheat was sown after soil was ploughed in early October and harvested in early June of the following year. Summer maize was directly sown in mid-June and harvested at the beginning of October each year. Before the next crop was sown the aboveground residues were removed from the soil surface. From the start year of the experiment to the sampling year in our study (1990 to 2014) the mean annual temperature was 15.2 °C and the mean annual precipitation was 628 mm. Further information on the soil properties is presented in Table 1 and climatic information during the experimental period is shown in Fig. S1. Evaporation, determined using the pan evaporation technique, fell below the detection limit from December to February. The irrigation rate at each of the growth stages in the winter wheat season (winter freeze, regreening-jointing, heading, and filling) was 600 m^3 ha^{-1} under drought conditions because a lack of precipitation would potentially suppress winter wheat growth.

2.2. Experimental design

The long-term field experiment comprised one unamended control (no fertilizer, CK) and two fertilization treatments in triplicate with the plots (each 45 m^2 in area) arranged in a randomized block design. The two fertilizer treatments were (1) chemical fertilizer application (NPK) and (2) combined application of manure and chemical fertilizer (MNPK). The fertilizer treatments provided an equivalent N application rate as shown in Table 2. The ratio of manure N to urea N was 7:3 in the wheat season. The chemical fertilizers applied were urea, triple superphosphate or calcium superphosphate, and potassium chloride, and the manure applied was cattle manure. The C and N concentrations in the manure were 310 and 25 g kg^{-1}. Fertilizer nitrogen (N) was split into basal and top-dressed fertilizer N. Phosphorus (P), potassium (K), and manure were applied as basal applications.

Firstly, soil aggregates in both 1990 and 2014 in the three treatments above were recovered by wet sieving using published standard methods (Elliott, 1986; Six et al., 2002a; Gulde et al., 2008). Secondly, in each treatment, field measured mean values of mass and C content in each aggregate fraction at the start (1990) and end (2014) of the experiment with a total of 24 data were used to calibrate the CAST model to determine the first-order rate constants for soil aggregate formation and disaggregation and for C mineralization in associated forms of SOC. The necessary calibration datasets were obtained through measured aggregate mass distribution and OC stocks in different aggregate size classes in the three treatments: control, NPK, and MNPK treatments. The CAST model simulation originally ran with historical data from 1990 for a period of 25 years. Thirdly, the calibrated model was then used for forward modeling, applying future climate change scenarios to the region of the field site in order to assess the potential impacts of climate and fertilizer practices on soil structure and its role in SOC accumulation and storage.

2.3.Soil sampling and analysis

Soil samples (0-20 cm depth) were taken from the long-term field experiment after the summer maize harvest in 2014 and compared with samples collected at the start of the experiment in October 1990. Soil samples were air-dried and stored at room temperature in sealed glass bottles.

Soil water-stable aggregate (WSA) separation was conducted by wet sieving according to Elliott (1986) and the macroaggregate fraction was further separated according to Six et al. (2002a). The scheme of aggregate fractionation is shown in Fig. S2 and details of the soil fractionation can be found in the supporting information. Briefly, the WSAs of bulk soil samples were separated into three size classes, namely macroaggregates (> 250 μm), free microaggregates (250 – 53 μm), and free silt-clays (< 53 μm) using the wet sieving method (Elliott, 1986). The efficiency of recovery during wet sieving averaged 98.3% (range 97.5-99.3%). Macroaggregates were separated into coarse POM (cPOM) (> 250 μm), microaggregates within macroaggregates (250 – 53 μm), and inter silt-clays (< 53 μm). The efficiency of recovery of this second step was 98.9% (range 96.2-99.9%). The isolation details of microaggregates within macroaggregates with heavy liquid fractionation can also be found in Gulde et al. (2008), and the microaggregates within macroaggregates fraction was separated into fine POM (fPOM), fine intra-POM (fiPOM), and intra silt-clays. After each fractionation step the separated soil fractions were oven-dried at 60 °C and weighed. The dried samples were passed through a 0.15-mm sieve and the C concentration was determined using a CN analyzer (Macrocube, Elementar, Hanau, Germany).

Soil texture was determined with a laser particle size analyzer (LS13320, Beckman Coulter, Brea, CA) following the approach by Yang et al. (2015). Soil total phosphorus (P), total potassium (K), Olsen-P, NH_4Ac-K, alkali-hydrolyzable N, and pH were determined by standard methods as described previously by Qiu et al. (2016).

2.4. Model description and aggregate C simulation

The CAST model has been widely used in the assessment of soil formation processes (Andrianaki et al., 2017), soil quality status under different environmental conditions and land use practices (Panakoulia et al., 2017), and the impacts of fertilization practices on changes in soil structure (Kotronakis et al., 2017; Li et al., 2017).

The CAST model divides soil WSAs into three size classes corresponding to macroaggregates, microaggregates and silt-clays (Fig. 1). According to Stamati et al. (2013), macroaggregates are formed by POM which is derived from plant litter fragmented by soil fauna and POM is then decomposed by microorganisms. The decomposing POM subsequently associates with silt-clay sized aggregates. Extracellular polymers of microbial origin provide cohesion between the structural components of aggregates and form both microaggregates and their incorporation with other textual units and aggregates within macroaggregates. Without continuous POM input, microbial activity decreases gradually as the C and energy resource is depleted with POM biodegradation, and the macroaggregates become unstable because of the lack of polymers of microbial origin. With new POM inputs, new macroaggregates form and the cycling of aggregation and disaggregation continues as fresh plant residues enter the soil.

The soil C dynamics within each aggregate size class of the CAST model are described by the RothC model (Coleman and Jenkinson, 1999). Briefly, the C pools in the RothC model are decomposable plant material (DPM), resistant plant material (RPM), microbial biomass (BIO), humified organic matter (HUM), and inert organic matter (IOM). In the CAST model, fresh plant litter is the initial POM and is split into DPM and RPM, and further, the DPM and RPM are treated as becoming physically fragmented by soil fauna to form the coarse fractions of DPM and RPM (cDPM, cRPM) and the fine fractions of DPM and RPM (fDPM, fRPM). In the aggregates in the CAST model, macroaggregates contain cDPM, cRPM, fDPM, fRPM, BIO, and HUM; microaggregates contain the same fractions as macroaggregates except for cDPM and cRPM. Silt and clay pools contain BIO and HUM. Each C pool in the three aggregate size classes decomposes by a first-order decay process with a specific rate constant and the decomposition rate of each C pool is determined by the three climatic factors temperature, precipitation, and evaporation through the effects on microbial activity as described for the Roth C model (Coleman and Jenkinson, 1999). The turnover rate of IOM ranges from centuries to millennia (Powlson et al., 2011) and IOM in the CAST models is resistant to decomposition. Regarding the measured C fractions in the CAST model, half of the C content in POM (POM-C) is partitioned into decomposable and resistant plant material, 5%

of the silt-clay fraction C is partitioned into BIO and the remaining silt-clay fraction C is partitioned into HUM (Stamati et al. 2013). All abbreviations used are summarized in Table S1.

Climatic conditions and crop C inputs throughout the experimental period together with basic soil properties, WSA size percentage, and organic C distribution in each aggregate size class at the start of the experiment were used as inputs for the CAST model, which runs on a monthly time step and simulates the top 20 cm of the soil profile. Climatic conditions were monthly mean temperature, monthly total precipitation and monthly total evaporation. The basic soil properties used were silt and clay content, bulk density, and soil depth. The WSA size percentages and their C contents at the beginning of the experiment are required as the initial conditions for aggregation (Coleman and Jenkinson, 1999; https://www.herslab.tuc.gr/downloads/cast-model).

The crop C input in the CAST model was simulated by the RothC model (version 2.1 for Windows) and the simulated C input rate was adjusted to match the change in SOC content from 1990 to 2014. RothC model-simulated crop C inputs are uniformly distributed each month during crop growth. The simulated crop C inputs were 0.305, 0.400 and 0.320 t C ha^{-1} $month^{-1}$ in the control, NPK and MNPK treatments from March to November during crop growth, and the manure C input of 1422 kg C ha^{-1} yr^{-1} in the MNPK treatment was added in October as shown in Table 2. The irrigation rate at the site during crop growth was treated as precipitation input in the CAST model (Stamati et al., 2013; Panakoulia et al., 2017). Further information on the CAST conceptual and mathematical model and parameter descriptions can be found in the supporting information.

2.5. Aggregate C predication under future climate scenarios

We used the Representative Concentration Pathway 2.6 scenario (RCP2.6) from the Climate Model Intercomparison Project Phase 5 (CMIP5) to implement the goals of the Paris Climate Agreement of 2015 (Rogelj et al., 2016). This Agreement seeks to limit the increase in global mean temperature to 1.5 or 2 °C by 2100 (Taylor et al., 2012; Burkett et al., 2014). We considered future climate projections by five General Circulation Models (GCMs) used in establishing RCP2.6, namely BCC-CSM1.1(m), BNUESM, EC-EARTH, IPSL-CM5A-LR and MRI-CGCM3 (Table S4, Fig. S3). These GCMs have been widely used in climate impact studies in China (Sabeerali et al., 2013; Chen and Frauenfeld, 2014; Miao et al., 2014) and provide outputs that can meet the data requirements to run the CAST model. The Taylor diagrams for five GCMs of temperature, precipitation, and evaporation are shown in Fig. S4.

Changes in soil structure and C stock in different aggregate size classes from 1990 to 2100 were simulated by driving the CAST model with climate data from the local meteorological station from 1990 to 2005 and the downscaled climate data from each GCM from 2006 to 2100. According to the IPCC (2014) the periods from 1986 to 2005 and from 2081 to 2100 are defined as the early 21st century and late 21st century, respectively. However, the early 21st century in the present study was defined as periods 1990 and 2005 because the field experiment began in 1990. For each GCM we calculated the difference in soil structure and C content in different aggregate classes from the early to the late 21st century by comparing the mean values in 2081-2100 to those in 1990-2005. During the above prediction the C input was maintained constant according to Chen et al. (2013).

2.6. Statistical analysis

Statistical analysis was conducted using the SPSS 16.0 for Windows software package. Prior to statistical analysis the data were checked for the normal distribution and homogeneity of variance. Data were $\log_{10}$- or power-transformed if they were not normally distributed. Mean values of variables in different aggregate size classes or SOC among treatments were compared using least significant difference at the 5% protection level. Mean values of predicted variables for the early 21st century and the later 21^{st} century were compared using independent-samples Student's t-test at the 5% level of probability.

3. Results

3.1 SOC

Measured and simulated SOC contents in 2014, annual C inputs, and measured SOC sequestration rates were all significantly ($P < 0.05$) different between treatments after 25 years of different fertilization treatments (1990-2014) (Table 3). The measured SOC in the NPK and MNPK treatments increased by 15.6 and 40.6% compared to the control. Both NPK and MNPK treatments increased SOC content from 1990 to 2014 but the control showed a decrease in SOC content over time (Table 3). The respective SOC contents in the control, NPK and MNPK treatments in 2014 increased by -6.1, 8.3 and 32.0% compared to values in 1990.

3.2 Aggregate mass and C content

The two fertilization treatments significantly ($P < 0.05$) decreased the percentage of mass contributed by silt-clay structural units in macroaggregates compared with the control (Table 4) with the opposite trend in the content of silt-clay structural units in the microaggregates within macroaggregates. The MNPK treatment significantly ($P < 0.05$) increased the percentage of silt-clay structural units in the microaggregates within macroaggregates and increased the content of coarse POM and fine POM in macroaggregates compared with the other two treatments (Table 4).

The MNPK treatment had the highest degree of aggregation with the largest macroaggregate C contents among the three treatments (Table 4). The two fertilization treatments significantly ($P < 0.05$) increased the C contents in microaggregates, microaggregates within macroaggregates, and silt-clay structural units in the microaggregates within macroaggregate particles compared with the control. The NPK treatment significantly ($P < 0.05$) decreased C contents in silt-clay structural units in macroaggregates compared with the control and the MNPK treatment, and MNPK had significantly ($P < 0.05$) higher C contents in macroaggregates and silt-clay structural units in the microaggregates within macroaggregates than the control or NPK. The microaggregate within macroaggregate C contents as a percentage of SOC stocks in NPK and MNPK were 20.4 and 23.4% representing the largest contributions of the carbon pools within the macroaggregate fractions.

3.3 Soil structure and SOC simulations

The baseline simulations for the experimental period 1990-2014 used the set of calibrated parameters and yielded the observed distribution of soil aggregates and C contents within aggregate fractions. The CAST model performed well (nRMSE < 13.3%, Table S3) overall when simulating the Fluvaquent soil (Fig. 1). The measured data at the start of the experiment in 1990 and those at the sampling date in 2014 captured the changes in water-stable aggregates percentage and OC stocks in the different aggregate size classes among the three treatments (Fig. 1).

Simulated SOC stocks in the NPK and MNPK treatments increased in tandem with the increase in the simulated microaggregate mass % (mass-microaggregate) and the organic C content in the microaggregate fractions (Fig. 1). Similarly, the increases in simulated organic C stocks in the macroaggregate fractions were mainly due to increases in the C contribution contained in silt-clay structural units in the microaggregates within macroaggregates and silt-clay structural units in macroaggregates. Since 1997 the C stocks in macroaggregates and silt-clay structural units in the microaggregates within macroaggregates reached saturation (Fig.1f, i) and the subsequent increase in SOC occurred mainly in the microaggregates in the MNPK treatment (Fig. 1f). There was less change in simulated OC stocks of coarse POM and fine POM than of the other fractions in the macroaggregate fractions (Fig. 1 g-i).

3.4 Predicted development of soil structure and SOC stocks

Under the different GCMs (Fig. 2) from 2006 to 2100 the predicted SOC stocks in the NPK and MNPK treatments gradually increased accompanied by an increase in OC stocks in microaggregates, an increase in microaggregate mass percentage and a decrease in macroaggregate mass percentage. Conversely, the predicted SOC in the control showed a slight increase accompanied by an increase in OC stocks in macroaggregate and macroaggregate mass percentage. With the sole exception of silt-clay structural units in the microaggregates within macroaggregates in the control, the macroaggregate fractions showed an increasing trend in organic C stocks in general.

The predicted WSA decrease in mass-silt-clay and increase in mass-microaggregate were strongest in the NPK treatment, the predicted WSA increase in mass-macroaggregate was strongest in the control, and the predicted WAS decrease in mass-macroaggregate was strongest in the MNPK treatment (Table 5).

The predicted changes in organic C stocks in different aggregate size classes differed significantly ($P < 0.05$) except for the OC content of the macroaggregates between the control and the NPK treatment (Table 5). The MNPK treatment significantly ($P < 0.05$) increased to 2.3 and 2.3 times the macroaggregate OC stocks over the control and the NPK treatment. The SOC and OC stocks in different aggregate fractions increased in all three treatments except for microaggregate OC stocks in the control. The changes in SOC stocks were derived mainly from the microaggregate OC stocks, and the changes in microaggregate OC stocks as a percentage of SOC stocks in the NPK and MNPK treatments were increases of 78.6 and 75.3%, respectively.

The MNPK treatment significantly increased the predicted changes in OC stocks associated with silt-clay structural units in the microaggregates within macroaggregates and fine POM compared with the control or NPK treatment (Table 5). The control treatment significantly increased OC stocks associated with silt-clay structural units in macroaggregates compared with the other two treatments. The predicted change in OC content of silt-clay structural units in the microaggregates within macroaggregates in the control showed a loss of C. Regarding the changes in OC stocks in the macroaggregate fractions the changes in cPOM OC stocks were not significantly different among the three treatments.

4. Discussion

4.1. Effects of fertilization practices on soil aggregates

SOC stocks can be increased by increasing soil C inputs (Gattinger et al., 2012; Zhang et al., 2015) and fertilizer application generally stimulates plant growth and promotes the transfer of photosynthetically-fixed C and crop residues into the soil (Brown et al., 2014). This may explain the significant increase in SOC in the NPK and MNPK treatments by 15.3 and 40.6% compared with the control in 2014 and the loss of SOC sequestration rate in the control from the start to 2014 at our site (Table 3). The accumulated SOC stocks in the NPK treatment was attributable to C inputs from crop residues and roots which increased with increasing N application rate up to the optimum N fertilization rate (Brown et al. 2014). Even so, SOC accumulation in the long term depended on the balance of C inputs and C outputs with SOC accumulation occurring when C inputs were higher than outputs, and SOC loss occurred when C inputs were lower than outputs (van Groenigen et al., 2006).

Carbon inputs from plant litter and manure application can affect aggregate formation and soil structure (Li et al., 2017) as shown by the 1.6 and 1.4 times ($P < 0.05$) higher C contents in macroaggregates in the MNPK treatment compared with the control and the NPK treatment in 2014 (Table 4). POM is the unprotected C derived from decomposed exogenous organic substrates and responds strongly to soil management practices (Gulde et al., 2008). A greater turnover rate of POM in macroaggregates (Gulde et al., 2008) results over time in a lower POM-C pool size compared with the other fractions in macroaggregates (Table 4, Fig. 1). In addition, the microbial decomposition of coarse POM provides the binding agents for soil clay- or silt-sized particles to form microaggregates within macroaggregates (Six et al., 2000b). Thus, the MNPK treatment had significantly ($P < 0.05$) higher C contents in microaggregates within macroaggregates than the NPK treatment or the control (Table 4). The NPK treatment also significantly increased microaggregates within macroaggregates compared with the control treatment due to the higher C input from greater plant productivity due to the fertilizer application, which was absent from the control (Table 3, 4). As Fig. 1 shows that the increase in C stocks in macroaggregates was derived mainly from an increase in C stock in microaggregates within macroaggregates. Moreover, the C stock in macroaggregates and microaggregates within macroaggregates reached saturation as time proceeded because both macroaggregates and microaggregates within macroaggregates remained stable from 1997.

Microaggregates are derived from both the fragmentation of macroaggregates and the association between organic molecules, soil silt-clay particles and cations (Six et al., 2004; Bronick and Lal, 2005). Macroaggregate fragmentation is attributed to the still decomposing POM, mechanical effects of tillage and environmental change (Six et al., 2004). Binding agents are derived mainly from the extracellular compounds of microbial metabolism or root exudation and exogenous substrates (Six et al., 2002b, 2004). In the MNPK treatment, sufficient C source application could promote microaggregates bound to form macroaggregates around the POM and resulted in a decrease in unbound microaggregates in the short term, then the OC stocks in microaggregates increased after the repeated C application (Figure 1f). Our measured results also indicate that the MNPK treatment had 1.4 times ($P < 0.05$) higher C contents in free microaggregates and 2.4 times higher C concentrations in microaggregates within macroaggregates than control, with a similar relationship between the NPK treatment and the control (Table 4). Numerous studies also report that application of organic soil amendments can increase microaggregate C contents compared with chemical fertilizers (Gulde et al., 2008; Chivenge et al., 2011).

The C content in < 53 μm soil particles is dominant in the organomineral complexes by chemical effects (Six et al., 2002b), including the free silt-clay particles, the silt-clay particles alone in the microaggregates within macroaggregates, and silt-clay particles in macroaggregates. Organic molecules derived from decomposed manure or plant residues can be associated with free silt-clay particles due to the relatively high particle specific surface area and increase in C content in free silt-clay particles. Furthermore, there is association between the free silt-clay particles and organic molecules forms microaggregates, macroaggregates, and microaggregates within macroaggregates when there is a sufficient supply of organic molecules (Six et al., 2002b; 2004), as shown by the significant ($P < 0.05$) increase of 1.3 times in C content in silt-clay within macroaggregates in the MNPK treatment compared with the NPK treatment and the significant ($P < 0.05$) increase of 2.2 and 1.8 times C content in silt-clay in microaggregates within macroaggregates in the MNPK and NPK treatments over the control (Table 4, Fig. 1).

4.2. Effect of climate change on soil structure

The forward simulations to 2100 predict how soil structure and SOC stocks and distribution between aggregate fractions will change with time. Under the RCP2.6 climate scenario, SOC stocks at our site were projected to increase over time (Fig. 2, S5; Table 5) even without manure or fertilizer applications. During the predication using the RCP2.6 climate scenario driving the CAST model the increase in soil moisture can be expected to be a major factor responsible for increasing SOC stocks in the control because the higher soil water content prevents soil warming and suppresses oxygen movement into the soil, further decreasing the rate of soil decomposition (Bronick and Lal, 2005). In each GCM the decrease in evaporation was much higher than the change in precipitation. The average evaporation decreased by 20.4 mm and the average precipitation increased by 0.55 mm in all GCM scenarios compared to those during 1990-2005 (Fig. S3). Here, the integrated effects of temperature and soil moisture on crop C inputs into the soil were not considered and the C input was assumed to remain unchanged. Chen et al. (2013) also reported that the increased yield potential in modern crop varieties can provide a trade off with the adverse effects of climate change. The increases in soil moisture were therefore more beneficial to soil structure development and SOC sequestration in the soil studied than the potentially adverse effects of increased SOC decomposition due to the increase in temperature (Fig. 2; Table 5).

Substantial soil environmental change can disrupt soil aggregates, decrease aggregate stability and expose the C to microorganisms (Bronick and Lal, 2005). Temperature increase generally promotes soil C mineralization at a global scale (Bond-Lamberty and Thomson, 2010). Low-molecular-weight compounds from microbial decomposition or root exudation provide the binding agents for soil aggregate formation that supports SOC accumulation (Tisdall and Oades, 1982; Bronick and Lal, 2005; Bhattacharyya et al., 2013). Under the RCP2.6 climate scenario the soil studied demonstrates the binding of silt-clay particles into microaggregates or macroaggregates and the fragmentation of macroaggregates into microaggregates, as shown by the negative mass values of different water-stable aggregates, especially in the fertilizer application treatments (Table 5). Moreover, the OC stocks in different aggregates increased among all the treatments on the whole (Fig. 2; Table 5). Overall, soil aggregate formation and SOC accumulation were promoted by the combined effects of environment factors, C inputs, and soil properties (Bronick and Lal, 2005; Huesh et al., 2017).

Under the RPC2.6 scenario, microaggregates are the main aggregate size class involved in changes in OC stocks and contribute the greatest mass among the size fractions of silt-clays, microaggregates and macroaggregates in the later 21st century (Table 5, Fig. 2, S5). Moreover, the change in free microaggregate OC stocks in all treatments was greatest among the aggregate size classes, and the OC stock in free microaggregates was 4.6 and 3.9 times that in microaggregates within macroaggregates (Fig. 2, S5; Table 5), although some studies report that microaggregates within macroaggregates are the dominant aggregate class to accumulate C stocks (Gulde et al., 2008; Brown et al., 2014). Soil tillage may be an important factor in our study as aggregate distribution shifted towards more free microaggregates and fewer macroaggregates with increasing cultivation intensity (Six et al., 2000b). This further confirms that SOC increase in the long term may be mainly derived from increasing free microaggregate C content in tilled soils (Gulde et al., 2008; Six et al., 2000b). Inconsistent with the second hypothesis, free microaggregates are predicted to be the primary aggregate classes contributing and protecting aggregate C in the tilled soil in our study (Fig. 2, S5; Table 5).

Poulton et al. (2017) report that SOC increased on average by 7‰ per year in surface soil (0-23 cm depth) in 65% of cases covering different fertilizer applications and land use changes, equivalent to a target accumulation rate of 4‰ per year at 0-40 cm soil depth for 20 years. Here, the projected rates of SOC accumulation in the control, NPK and MNPK treatments from the early to the later 21st century under the RCP2.6 scenario are 0.5, 6.7, and 12.0‰, respectively. These results suggest that appropriate fertilizer additions to SOC storage would help to meet the goals of the "4 per 1000 initiative" under the RCP2.6 scenario, although this does not consider other potentially negative processes such as nitrous oxide emissions and nitrate leaching (Baveye et al., 2018). In fact, optimum agronomic management practices, especially the combination of manure and chemical fertilizers, can effectively decrease emissions of trace gases in Fluvaquent soils on the North China Plain (Meng et al., 2005; Qiu et al., 2012; Cui et al., 2013; Huang et al., 2017; Lugato et al. 2018) which account for 27% of the entire arable land area in China (Han et al., 2018), suggesting the presence of a substantial potential SOC sink for atmospheric CO_2 under the RCP2.6 scenario.

5. Conclusions

Sufficient C inputs to soil can promote silt-clay particle binding to microaggregates and macroaggregates and increase the C contents in microaggregates and macroaggregates as shown by the significantly ($P < 0.05$) highest macroaggregate C content in the MNPK treatment compared to the other experimental treatments. Even so, the C content in free microaggregates was higher than that in microaggregates within macroaggregates in our three treatments. Our results further suggest that Fluvaquent soils can be substantial C sinks under the RCP2.6 scenario and that free microaggregates are the main soil fraction contributing to future SOC sequestration. In general, the use of mathematical process modeling coupled with soil structure and carbon dynamics has the potential to generate further insights into (1) the potential C sink of Fluvaquent soils in future climate change and (2) the dominant effects of free microaggregates in C stocks in Fluvaquent soils in the current tillage for the annual double cropping systems of wheat and maize. Future studies will strengthen evidence on the further optimization of agronomic practices in addition to fertilization combined with other RCP scenarios to explore the differences in physical protection of SOC stocks by soil aggregates in different soil types and cropping systems.

Acknowledgements

We are very grateful for the valuable suggestions and modifications made by Kees Jan van Groenigen. This study was supported by the National Key Research and Development Plan (2016YFD0200101, 2018YFD0200804), the Fundamental Research Funds for Central Non-Profit Scientific Institutions (1610132019014), and Taishan Scholars Project Special Funding. Shaojun Qiu received funding from the Chinese Scholarship Council for a twelve-month fellowship at the University of Leeds, UK, during which part of this study was completed.

References

Andrianaki, M., Bernasconi, S.M., Nikolaidis, N.P. 2017. Quantifying the Incipient Development of Soil Structure and Functions Within a Glacial Forefield Chronosequence Advances in Agronomy, 142, 215-239.

Apostolakis, A., Panakoulia, S., Nikolaidis, N.P., Paranychianakis, N.V. 2017. Shifts in soil structure and soil organic matter in a chronosequence of setaside fields. Soil Tillage Research, 174, 113–119.

Averill, C., Waring, B. 2018. Nitrogen limitation of decomposition and decay: How can it occur?

Global Change Biology, 24, 1417–1427.
Baveye, P.C., Berthelin, J., Tessier, D., Lemaire, G. 2018. The “4 per 1000” initiative: A credibility issue for the soil science community? Geoderma, 309, 118–123.
Banwart, S.A., Nikolaidis, N.P., Zhu, Y.-G., Peacock, C.L., Sparks, D.L. 2019. Soil functions: connecting Earth's critical zone. Annual Review of Earth and Planetary Sciences, 47, 333–359.
Bond-Lamberty, B., Thomson, A. 2010. A global database of soil respiration data. Biogeosciences, 7, 1915–1926.
Bhattacharyya, R., Pandey, S.C., Bisht, J.K., Bhatt, J.C., Gupta, H.S., Tuti, M.D., Mahanta, D., Mina, B.L., Singh. R.D., Chandra, S., Srivastva, A.K., Kundu, S. 2013. Tillage and irrigation effects on soil aggregation and carbon pools in the Indian sub-himalayas. Agronomy Journal, 105:101–112.
Bronick, C.J., Lal, R. 2005. Soil structure and management: a review. Geoderma, 124, 3–22.
Brown, K.H., Bach, E.M., Drijber, R.A., Hofmockel, K.S., Jeske, E.S., Sawyer, J.E., Castellano, M.J. 2014. A long-term nitrogen fertilizer gradient has little effect on soil organic matter in a high-intensity maize production system. Global Change Biology, 20, 1339–1350.
Carvalhais, N., Forkel, M., Khomik, M., Bellarby, J., Jung, M., Migliavacca, M., Mu, M.Q., Saatchi, S., Santoro, M., Thurner, M., Weber, U., Ahrens, B., Beer, C., Cescatti, A., Randerson, J.T., Reichstein, M. 2014. Global covariation of carbon turnover times with climate in terrestrial ecosystems. Nature, 514, 213–217.
Chabbi, A., Lehmann, J., Ciais, P., Loescher, H. W., Cotrufo, M. F., Don, A., SanClements, M., Schipper, L., Six, J., Simth, P., Rumpel, C. 2017. Aligning agriculture and climate policy. Nature Climate Change, 7, 307–309.
Chen, L., Frauenfeld, O.W. 2014. A comprehensive evaluation of precipitation simulations over China based on CMIP5 multimodel ensemble projections. Journal of Geophysical Research

Atmospheres, 119, 5767–5786.

Chen, X., Chen, F., Chen, Y., Gao, Q., Yang, X., Yuan, L., Zhang, F., Mi, G. 2013. Modern maize hybrids in Northeast China exhibit increased yield potential and resources use efficiency despite adverse climate change. Global Change Biology, 19, 923–936.

Chivenge, P., Vanlauwe, B., Gentile, R., Six, J. 2011. Comparison of organic versus mineral resource effects on short-term aggregate carbon and nitrogen dynamics in a sandy soil versus a fine textured soil. Agriculture, Ecosystems and Environment, 140, 361–371.

Coleman, K., Jenkinson, D.S. 1999. RothC-26.3—a model for the turnover of carbon in soil: model description and windows users guide. Lawes Agricultural Trust, Harpenden. ISBN: 0-951-4456-8-5. November 1999 issue.

Cui, Z., Yue, S., Wang, G., Meng, Q., Wu, L., Yang, Z., Zhang, Q., Li, S., Zhang, F., Chen, X. 2013. Closing the yield gap could reduce projected greenhouse gas emissions: a case study of maize production in China. Global Change Biology, 19, 2467–2477.

Elliott ET. 1986. Aggregate structure and carbon, nitrogen, and phosphorus in native and cultivated soils. Soil Science Society of America Journal, 50, 627–633.

Dou, X., He, P., Zhu, P., Zhou, W. 2016. Soil organic carbon dynamics under long-term fertilization in a black soil of China: Evidence from stable C isotopes. Scientific Reports, 6, e21488.

Francaviglia, R., Soleimani, A., Bavani, A.R.M., Hosseini, S.M., Jafari, M. 2020. Probability assessment of climate change impacts on soil organic carbon stocks in future periods: a case study in Hyrcanian forests (Northern Iran). European Journal of Forest Research, 139, 1-16.

Gattinger, A., Muller, A., Haeni, M., Skinner, C., Fliessbach, A., Buchmann, N., Mäder, P., Stolze, M., Smith, P., Scialabba, N.E., Niggli, U. 2012. Enhanced top soil carbon stocks under organic farming. PNAS, 109, 18226–18231.

Gulde, S., Chung, H., Amelung, W., Chang, C., Six, J. 2008. Soil carbon saturation controls labile and stable carbon pool dynamics. Soil Science Society of America Journal, 72, 605–612.

Han, D., Wiesmeier, M., Conant, R.T., Kühnel, A., Sun, Z., Kögel-Knabner, I., Hou, R., Cong, P., Liang, R., Ouyang, Z. 2018. Large soil organic carbon increase due to improved agronomic management in the North China Plain from 1980s to 2010s. Global Change Biology, 24, 987–1000.

He, Y.T., Zhang, W.J., Xu, M.G., Tong, X.G., Sun, F.X., Wang, J.Z., Huang, S.M., Zhu, P., He, X.H. 2015. Long-term combined chemical and manure fertilizations increase soil organic carbon and total nitrogen in aggregate fractions at three typical cropland soils in China. Science of the Total Environment, 532, 635–644.

Huang, T., Hu, X., Gao, B., Yang, H., Huang, C., Ju, X. 2018. Improved Nitrogen Management as a Key Mitigation to Net Global Warming Potential and Greenhouse Gas Intensity on the North China Plain. Soil Science Society of America Journal, 82, 136–146.

Huang, Y., Sun, W.J. 2006. Changes in topsoil organic carbon of croplands in mainland China over the last two decades. Chinese Science Bullin, 51, 1785–1803.

Huesh, A., Bakkantyne, A., Cooper, L., Manera, M., Kimball, J., Watts, J. 2017. The sensitivity of soil respiration to soil temperature, moisture, and carbon supply at the global scale. Global Change Biology, 23, 2090–2103.

Jiang, G., Xu, M., He, X., Zhang, W., Huang, S., Yang, X., Liu, H., Peng, C., Shirato, Y., Lizumi, T., Murphy, D.V. 2014. Soil organic carbon sequestration in upland soils of northern China under variable fertilizer management and climate change scenarios. Global Biogeochemistry Cycles, 28, 319–333.

IPCC, 2014. Climate Change 2014: Impacts, Adaptation, and Vulnerability. Part A: Global and Sectoral Aspects. Contribution of Working Group II to the Fifth Assessment Report of the Intergovernmental Panel on Climate Change. Cambridge University Press, Cambridge, UK.

Keating, B.A., Carberry, P.S., Hammer, G.L., Probert, M.E., Robertson, M.J., Holzworth, D., Huth, N.I., Hargreaves, J.N.G., Meinke, H., Hochman, Z., McLean, G., Verburg, K., Snow, V., Dimes, J.P., Silburn, M., Wang, E., Brown, S., Bristow, K.L., Asseng, S., Chapman, S., McCown, R.L., Freebairn, D.M., Smith, C.J. 2003. An overview of APSIM, a model designed for farming systems simulation. European of Journal Agronomy, 18, 267–288.

Kotronakis, M., Giannakis, G.V., Nikolaidis, N.P., Rowe, E.C., Valstar, J., Paranychianakis, N.V., Banwart, S.A. 2017. Modeling the Impact of Carbon Amendments on Soil Ecosystem Functions Using the 1D-ICZ Model. Advances in Agronomy, 142, 315-352.

Li, N., You, M.Y., Zhang, B., Han, X.Z., Panakoulia, S.K., Yuan, Y.R., Liu, K., Qiao, Y.F., Zou, W.X., Nikolaidis, N.P., Banwart, S.A. 2017. Modeling soil aggregation at the early pedogenesis stage from the parent material of a Mollisol under different agricultural practices. Advances in Agronomy, 142, 181–214.

Lugato, E., Leip, A., Jones A. 2018. Mitigation potential of soil carbon management overestimated by neglecting N_2O emissions. Nature Climate Change, 8, 219–223.

Malamoud, K., McBratney, A.B., Minasny, B., Field, D.J. 2009. Modelling how carbon affects soil structure. Geoderma 149, 19–26.

Meng, L., Ding, W., Cai, Z. 2005. Long-term application of organic manure and nitrogen fertilizer on N_2O emissions, soil quality and crop production in a sandy loam soil. Soil Biology and Biochemistry, 37, 2037–2045.

Miao, C., Duan, Q., Sun, Q., Huang, Y., Kong, D., Yang, T., Ye, A., Di, Z., Gong, W. 2014. Assessment of CMIP5 climate models and projected temperature changes over Northern Eurasia. Environmental Research Letter, 9, e55007

Panakoulia, S.K., Nikolaidis, N.P., Paranychianakis, N.V., Menon, M., Schiefer, J., Lair, G.J., Krám, P., Banwart, S.A. 2017. Factors controlling soil structure dynamics and carbon sequestration across different climatic and lithological conditions. Advances in Agronomy,

142, 241–276.
Poulton, P., Johnston, J., Macdonald, A., White, R., Powlson, D. 2018. Major limitations to achieving “4 per 1000” increases in soil organic carbon stock in temperate regions: evidence from long-term experiments at Rothamsted Research, United Kingdom. Global Change Biology, 24, 2563–2584.
Powlson, D.S., Whitmore, A.P., Goulding, K.W.T. 2011. Soil carbon sequestration to mitigate climate change: a critical re-examination to identify the true and the false. European Journal of Soil Science, 62, 42–55.
Qiu, S., Gao, H., Zhu, P., Hou, Y., Zhao, S., Rong, X., Zhang, Y., He, P., Christie, P., Zhou, W. 2016. Changes in soil carbon and nitrogen pools in a Mollisol after long-term fallow or application of chemical fertilizers, straw or manures. Soil Tillage Research, 163, 255–265.
Qiu, S., Ju, X., Lu, X., Li, L., Ingwersen, J., Streck, T., Christie, P., Zhang, F. 2012. Improved nitrogen management for an intensive winter wheat / summer maize double-cropping system. Soil Science Society of American journal, 76, 286–297.
Rogelj, J., den Elzen, M., Höhne, N., Fransen, T., Fekete, H., Winkler, H., Schaeffer, R., Sha, F., Riahi, K., Meinshausen, M. 2016. Paris Agreement climate proposals need a boost to keep warming well below 2 °C. Nature, 534, 631–639.
Russell, A.E., Cambardella, C.A., Laird, D.A., Jaynes, D.B., Meek, D.W. 2009. Nitrogen fertilizer effects on soil carbon balances in midwestern U.S. agricultural systems. Ecological applications, 19, 1102–1113.
Sabeerali, C.T., Ramu, D.A., Dhakate, A., Salunke, K., Mahapatra, S., Rao, S.A. 2013. Simulation of boreal summer intraseasonal oscillations in the latest CMIP5 coupled GCMs. Journal of Geophysical Research Atmospheres, 118, 4401–4420.
Six, J., Bossuyt, H., Degryze, S., Denef, K. 2004. A history of research on the link between (micro)aggregates, soil biota, and soil organic matter dynamics. Soil Tillage Research, 79,

7-31.

Six, J., Callewaert, P., Lenders, S., De Gryze, S., Morris, S. J., Gregorich, E.G., Paul, E.A., Paustian K. 2002a. Measuring and Understanding Carbon Storage in Afforested Soils by Physical Fractionation. Soil Science Society of American Journal, 66: 1981–1987.

Six, J., Paustian, K. 2014. Aggregate-associated soil organic matter as an ecosystem property and a measurement tool. Soil Biology and Biochemistry, 68, A4–A9.

Six, J., Conant, R.T., Paul, E.A., Paustian, K. 2002b. Stabilization mechanisms of soil organic matter: Implications for C-saturation of soils. Plant and Soil, 241,155–176.

Six, J., Elliott, E.T., Paustian, K. 2000a. Soil macroaggregate turnover and microaggregate formation: a mechanism for C sequestration under no-tillage agriculture. Soil Biology and Biochemistry, 32, 2099–2103.

Six, J., Paustian, K., Elliott, E.T., Combrink, C. 2000b. Soil Structure and Organic Matter: I. Distribution of Aggregate-Size Classes and Aggregate-Associated Carbon. Soil Science Society of American Journal, 64:681–689.

Stamati, F.E., Nikolaidis, N.P., Banwart, S., Blum, W.E.H. 2013. A coupled carbon, aggregation, and structure turnover (CAST) model for topsoils. Geoderma, 211–212, 51-64.

Taylor, K.E., Stouffer, R.J., Meehl, G.A. 2012. An Overview of CMIP5 and the Experiment Design. Bulletin of American Meteorological Society, 93, 485-498.

Tisdall, J.M., Oades, J.M. 1982. Organic matter and water-stable aggregates in soils. European Journal of Soil Science, 33, 141–163.

Treseder, K.K. 2008. Nitrogen additions and microbial biomass: a meta-analysis of ecosystem studies. Ecology Letters, 11, 1111–1120.

Valkama, E., Gulya Kunypiyaeva, G., Zhapayev R., Karabayev, M., Zhusupbekov, E., Perego, A., Schillaci, C., Sacco, D., Barbara Moretti, B., Carlo Grignani C., Acutis, M. 2020. Can conservation agriculture increase soil carbon sequestration? A modelling approach.

Geoderma, 369, 114298.

Van Gestel, N., Shi, Z., Van Groenigen, K.J., Osenberg, C.W., Andresen, L.C., Dukes, J.S., Hovenden, M.J., Luo, Y., Michelsen, A., Pendall, E. and Reich, P.B. 2018. Predicting soil carbon loss with warming. Nature, 554, E4–E5.

van Groenigen, K.J., Six, J., Hungate, B.A., de Graaff, M.-A., van Breemen, N., van Kessel, C. 2006. Element interactions limit soil carbon storage. PNAS, 103, 6571–6574.

Yan, Y., Tian, J., Fan, M., Zhang, F., Li, X., Christie, P., Chen, H., Lee, J., Kuzyakov, Y., Six, J. 2012. Soil organic carbon and total nitrogen in intensively managed arable soils. Agriculture, Ecosystems and Environment, 150, 102– 110.

Yang, X.L., Zhang, Q.Y., Li, X.Z., Jia, X.X., Wei, X.R., Shao, M.A. 2015. Determination of soil texture by laser diffraction method. Soil Science Society of America Journal, 79, 1556–1566.

Zhang, K., Dang, H., Zhang, Q., Cheng, X. 2015. Soil carbon dynamics following land-use change varied with temperature and precipitation gradients: evidence from stable isotopes. Global Change Biology, 21, 2762–2772.

Zhou, X., Xu, X., Luo, Y. 2018. Temperature sensitivity of soil organic carbon decomposition increased with mean carbon residence time: Field incubation and data assimilation. Global Change Biology, 24, 810–822.

Zhang, X., Xu, M., Sun, N., Xiong, W., Huang S., Wu, L. 2016. Modelling and predicting crop yield, soil carbon and nitrogen stocks under climate change scenarios with fertiliser management in the North China Plain. Geoderma, 265, 176–186.

Figure captions

Fig. 1 Water-stable aggregates (% mass), soil organic carbon (SOC) stock distribution (t ha^{-1}), and macroaggregate OC stock distribution (t ha^{-1}) as affected by fertilizer treatment in control (CK), chemical fertilizer (NPK), and combined manure and chemical fertilizer (MNPK) treatments in a Fluvaquent soil with CAST model simulation.

Aggregate symbols in legend: see Table 4 footnote.

Crosses in the Figure are the measured values of the samples at the start of the experiment (1990) and in 2014; the time series of plots x-axis between the two crosses in each curve are for the period 1990-2014.

Fig. 2 Trends in predicted water-stable aggregates (% mass), soil organic carbon (SOC) stock distribution (t ha^{-1}), and macroaggregate OC stock distribution (t ha^{-1}) at 0-20 cm soil depth for five General Circulation Models of the RCP2.6 scenario from 2006-2010 to the late 21st century (2081-2100) with CAST model simulation in control (CK), chemical fertilizer (NPK), and combined manure and chemical fertilizer (MNPK) treatments in a Fluvaquent soil.

For aggregate symbols, see Table 4 footnote.

The x-axis scale main divisions show five-yearly intervals and the subdivisions show yearly intervals (n = 475).

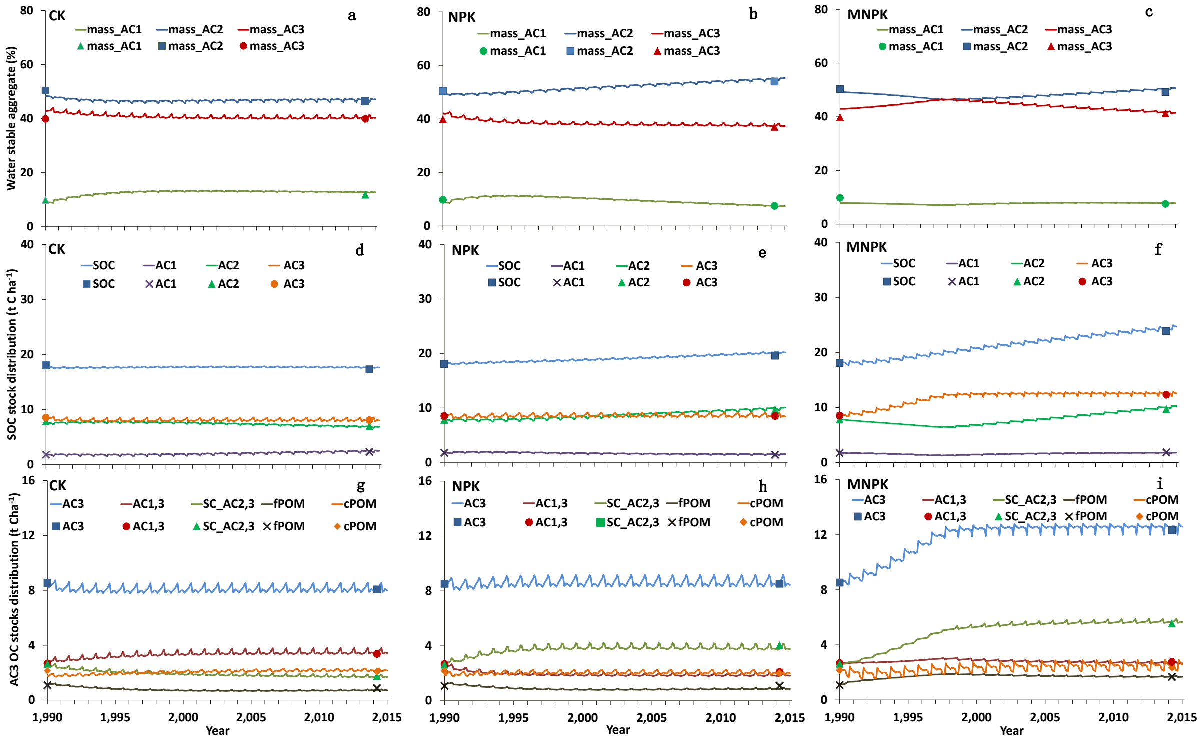
CK
a
mass_AC1
mass_AC2
mass_AC3
NPK
b
MNPK
c
Water stable aggregate (%)
CK
d
SOC
AC1
AC2
AC3
NPK
e
MNPK
f
SOC stock distribution (t C ha-1)
CK
g
AC3
AC1,3
SC_AC2,3
fPOM
cPOM
NPK
h
MNPK
i
AC3 OC stocks distribution (t Cha-1)
1,990
1,995
2,000
2,005
2,010
2,015
Year

Fig. 1

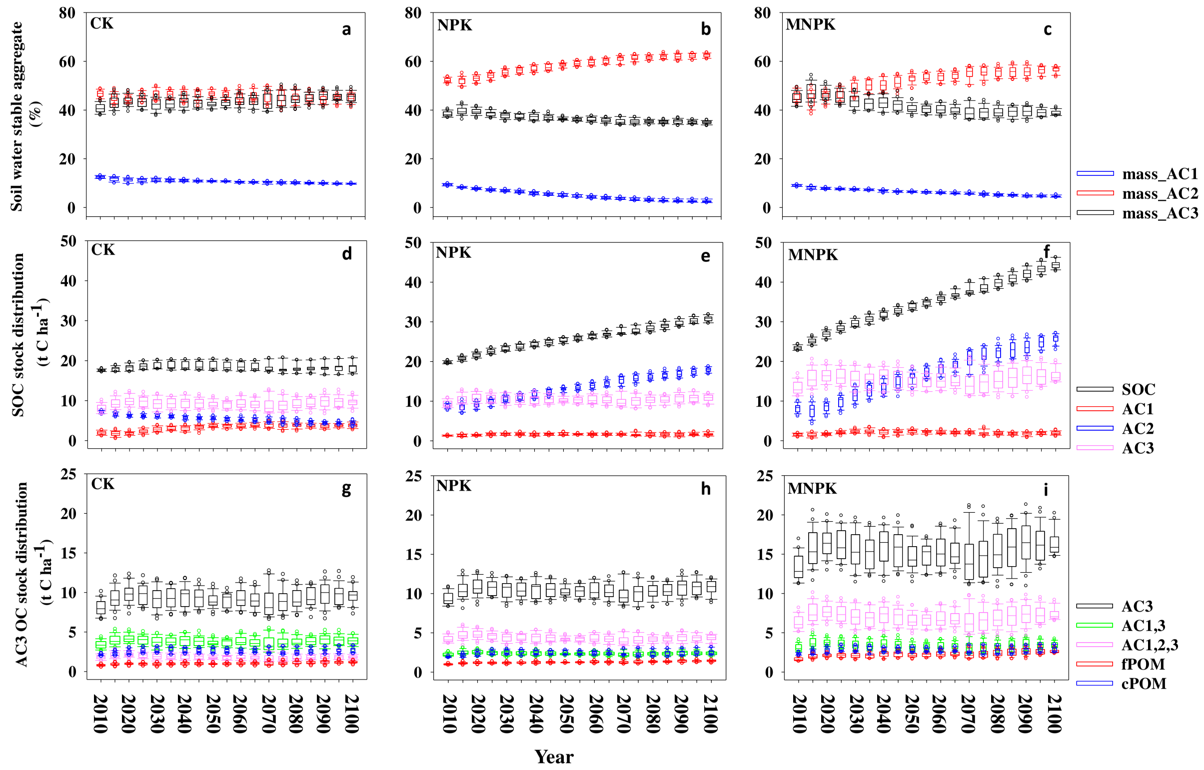
Soil water stable aggregate (%)
SOC stock distribution (t C ha-1)
AC3 OC stock distribution (t C ha-1)
CK
NPK
MNPK
a
b
c
d
e
f
g
h
i
mass_AC1
mass_AC2
mass_AC3
SOC
AC1
AC2
AC3
AC1,3
AC1,2,3
fPOM
cPOM
Year

Fig. 2

Table 1 Soil properties in the top 20 cm of the soil profile at the start year of the field experiment (1990).

Soil property	Value	Soil property	Value
pH	8.3 ± 0.02	Olsen-P (kg ha^{-1})	17.6 ± 0.16
Soil organic C (t ha^{-1})	18.0 ± 0.54	NH_4Ac-K (kg ha^{-1})	201.1 ±0.35
Total N (t ha^{-1})	1.9 ± 0.08	Soil texture	
Total P (t ha^{-1})	1.6 ± 0.05	Sand (%)	62.1±0.61
Total K (t ha^{-1})	45.6 ± 0.38	Clay (%)	10.3±0.23
Alkali-hydrolyzable N (kg ha^{-1})	206.8 ± 0.46	Silt (%)	27.6±0.10

Table 2 Fertilizer rates in the control (CK), chemical fertilizer (NPK), and combined manure and chemical fertilizer (MNPK) treatments for each crop. Unit, kg ha^{-1} yr^{-1}

Crop	CK	NPK	MNPK		
	N:P:K	N:P:K*	N:P:K	Manure N	Manure C
Wheat	0:0:0	165:36:68	50:36:68	115	1422
Maize	0:0:0	188:40:78	188:40:78	0	0

*, fertilizers applied are chemical fertilizers and do not include manure nutrients.

Table 3 Measured SOC contents in 2014 and SOC sequestration rates, as well as simulated SOC contents in 2014, and annual C inputs in the control (CK), chemical fertilizer (NPK), and combined manure and chemical fertilizer (MNPK) treatments.

	Measured SOC (t ha^{-1})	Simulated SOC (t ha^{-1})	Annual C inputs (t C ha^{-1} yr^{-1})	Measured SOC sequestration rate* (kg ha^{-1} yr^{-1})
CK	17.0±0.5c	17.0±0.4c	1.4±0.1c	-45.0[§]±8.6c
NPK	19.6±0.9b	19.5±0.9b	2.0±0.2b	59.5±13.8b
MNPK	23.9±0.1a	23.6±0.1a	2.9±0.03a	230.7±19.2a

Mean values followed by a different letter within a column are different at $P < 0.05$.

* SOC sequestration rate is the difference in measured SOC between 1990 and 2014 divided by the number of years (25).

§ A negative value shows C loss.

Table 4 Water-stable aggregate percentage and content at 0-20 cm soil depth in control (CK), chemical fertilizer (NPK), and combined manure and chemical fertilizer (MNPK) treatments in 2014.

	Treatment	Mass_AC1[#]	Mass_AC2	Mass_AC3 (AC3)	AC2,3	AC1,3	AC1,2,3	cPOM	fPOM
Percentage	CK	11.7[†]±1.5a[‡]	46.4±2.5b	39.8±1.2a	21.6±1.4b	13.8±0.9a	13.2±0.8c	0.29±0.04b	0.14±0.01b
(%)	NPK	7.5±0.3a	54.0±1.2a	37.0±1.8a	24.0±0.9ab	9.1±0.8b	17.5±0.2b	0.26±0.02b	0.22±0.003b
	MNPK	7.5±1.4a	49.3±0.3ab	41.2±1.6a	27.2±1.1a	10.0±0.4b	20.1±0.6a	0.39±0.001a	0.32±0.01a
C content	CK	2.3±0.4a	7.0±0.2b	7.8±0.6b	2.6±0.3c	3.4±0.4a	1.7±0.2c	2.1±0.2a	0.9±0.1a
($t\ ha^{-1}$)	NPK	1.4±0.1a	9.7±0.7a	8.5±0.6b	4.0±0.2b	2.1±0.1b	3.1±0.1b	2.0±0.2a	1.1±0.1a
	MNPK	1.9±0.4a	9.7±0.3a	12.3±0.2a	5.6±0.4a	2.8±0.2a	3.8±0.3a	2.3±0.1a	1.7±0.1a

[#]AC3, macroaggregates (> 250 μm); AC2, free microaggregates (250-53 μm); AC1, free silt-clay (< 53 μm);
AC2,3, microaggregates within macroaggregates (250-53 μm); AC1,3, silt-clay structural units in macroaggregates (< 53 μm);
AC1,2,3, silt-clay structural units in microaggregates within macroaggregates (< 53 μm);
cPOM, coarse particulate organic matter in macroaggregate; fPOM, fine particulate organic matter in macroaggregate;
[†] Mean of three replicates.
[‡] Mean values followed by a different letter within a column for percentage or content are different at $P < 0.05$.

Table 5 Predicted differences in soil structure and organic C stocks in different aggregate size classes for late 21st century (2081-2100) in control (CK), chemical fertilizer (NPK), and combined manure and chemical fertilizer (MNPK) treatments under RCP2.6 scenario relative to early 21st century (1990-2005).

Treatment	Water-stable aggregates (%)			SOC stock distribution (t ha^{-1})				Macroaggregate organic C stock distribution (t ha^{-1})					
	Mass_AC1	Mass_AC2	Mass_AC3	SOC	AC1	AC2	AC3	AC3	AC2,3	AC1,3	AC1,2,3	fPOM	cPOM
CK	-1.8*±1.38a#	-3.0±0.78c	4.8±1.26a	0.9±0.19c	1.9±0.20a	-3.4±0.23c	2.2±0.57b	2.2±0.57b	0.05±0.41c	1.0±0.28a	-0.2±0.24c	0.2±0.18c	1.1±0.19a
NPK	-7.8±0.92c	12.0±0.76a	-4.2±1.36b	11.7±0.49b	0.005±0.15c	9.2±0.38b	2.2±0.41b	2.2±0.41b	1.0±0.18b	0.2±0.22c	0.6±0.32b	0.4±0.18b	1.0±0.21a
MNPK	-4.1±0.84b	10.1±1.10b	-6.0±0.80c	22.7±0.87a	0.3±0.14b	17.1±0.96a	5.1±0.81a	5.1±0.81a	3.2±0.66a	0.6±0.13b	2.2±0.74a	1.0±0.17a	1.2±0.29a

For symbols see Table 4 footnote.

* Mean of the five climate scenarios; values calculated by the difference between the late 21st century and early 21st century; C stock in AC2,3 was the sum of AC1,2,3 and fPOM.

Mean values followed by a different letter within a column are different at $P < 0.05$.